

M_{BH} - relation in SDSS flat-spectrum radio quasars

Minfeng Gu^{1?}, Zhaoyu Chen^{1,2}, Xinwu Cao¹

¹ Key Laboratory for Research in Galaxies and Cosmology, Shanghai Astronomical Observatory, Chinese Academy of Sciences, 80 Nandan Road, Shanghai 200030, China

² Graduate School of the Chinese Academy of Sciences, Beijing 100039, China

2 April 2024

ABSTRACT

The relationship between the black hole mass and velocity dispersion indicated with [O III] line width is investigated for a sample of 87 flat-spectrum radio quasars (FSRQs) selected from SDSS DR3 quasar catalogue. We found the $M_{\text{bh}} - \sigma_{\text{[O III]}}$ relation is deviated from Tremaine et al. relation for nearby inactive galaxies, with a larger black hole mass at given velocity dispersion. There is no strong evidence of cosmology evolution in $M_{\text{bh}} - \sigma_{\text{[O III]}}$ relation up to $z \approx 0.8$. A significant correlation between the [O III] luminosity and Broad Line Region (BLR) luminosity is found. When transferring the [O III] luminosity to Narrow Line Region (NLR) luminosity, the BLR luminosity is, on average, larger than NLR one by about one order of magnitude. We found a strong correlation between the synchrotron peak luminosity and NLR luminosity, which implies a tight relation between the jet physics and accretion process.

Key words: black hole physics – galaxies: active – galaxies: nuclei – quasars: emission lines – quasars: general

1 INTRODUCTION

The evolution of black holes has been shown to be closely coupled to that of their host galaxies for normal galaxies, mainly through the tight correlation between the central black hole mass and the bulge mass and luminosity (Kormendy & Richstone 1995; Magorrian et al. 1998), and tighter one between the central black hole mass and stellar velocity dispersion in the galactic bulge (Ferrarese & Merritt 2000; Gebhardt et al. 2000a). The latter relation has been established by Tremaine et al. (2002) for a sample of 31 nearby inactive galaxies as

$$\log \left(\frac{M_{\text{BH}}}{M_{\odot}} \right) = (8.13 \pm 0.06) + (4.02 \pm 0.32) \log \left(\frac{\sigma}{200 \text{ km s}^{-1}} \right) \quad (1)$$

For some AGNs with available bulge velocity dispersion and the reverberation mapping black hole mass, Gebhardt et al. (2000b) and Ferrarese et al. (2001) found that these AGNs also follow the $M_{\text{bh}} - \sigma$ relation founded in the nearby inactive galaxies. With the aim to constrain the nature and evolution of AGNs and the advantage of relative higher redshift of AGNs, the $M_{\text{bh}} - \sigma$ relation and its evolution have been extensively explored for different AGN populations, such as radio-quiet, radio-loud AGNs, narrow line Seyfert I galaxies and young radio galaxies et al. (e.g. Shields et al. 2003; Bian & Zhao 2004; Bonning et al. 2005; Liu & Jiang 2006; Salviander et al. 2007; Bian et al. 2008; Shen et al. 2008; Wu

2009a), however it is still in large debates whether AGNs generally follow the $M_{\text{bh}} - \sigma$ relation.

While the derivation of M_{bh} from AGNs broad line widths and continuum (and/or broad line) luminosity is now well established (e.g. Kaspi et al. 2000; Greene & Ho 2005; Kong et al. 2006), the measurements of σ are generally difficult for quasars, due to the faintness of the host galaxy and the relative brightness of active nucleus. When stellar velocities dispersion cannot be measured, the line widths of the narrow emission lines (e.g. [O III], [S II]) usually can be used to trace σ (Nelson & Whittle 1996; Greene & Ho 2005). Nelson & Whittle (1996) compared the bulge magnitudes, [O III] $\lambda 5007$ line widths, and stellar velocity dispersions in Seyfert galaxies, adopting $\sigma_{\text{[O III]}} = F W_{\text{HM}}(\text{[O III]})/2.35$, and found, on average, good agreement between $\sigma_{\text{[O III]}}$ and σ , although $\sigma_{\text{[O III]}}$ shows more scatter than σ on a Faber-Jackson plot. This implies that the kinematics of narrow-line region (NLR) gas is largely dominated by the bulge gravitational potential, therefore, can be effectively used as a substitute for σ of galaxy bulges. Using [O III] line width as surrogates for σ , Nelson (2000) claimed that the $M_{\text{bh}} - \sigma_{\text{[O III]}}$ relation for normal galaxies and active galactic nuclei is preserved. Albeit some defect of [O III] line profile (e.g. asymmetry and non-Gaussian) and other surrogates proposed (e.g. [S II], Greene & Ho 2005), the width of [O III] is still most commonly used as surrogate for σ in AGNs (e.g. Bonning et al. 2005; Bian et al. 2008).

The formation of radio jets is still an unresolved issue in AGNs research. While radio-quiet AGNs roughly follow the $M_{\text{bh}} - \sigma$ relation of normal galaxies, radio-loud ones deviate, in the sense

? gumf@shao.ac.cn

that radio-loud objects have, on average, larger black hole mass than radio-quiet objects for a given velocity dispersion (e.g. Bian & Zhao 2004; Bonning et al. 2005; Liu & Jiang 2006; Salviander et al. 2007; Bian et al. 2008; Shen et al. 2008). Among the population of radio-loud AGNs, FSRQs represent an extreme class, which are generally characterized by strong and rapid variability, high polarization, and apparent superluminal motion. These extreme properties are generally interpreted as a consequence of non-thermal emission from a relativistic jet oriented close to the line of sight. In this letter, we investigate the relationship between the black hole mass and $\sigma_{\text{[O III]}}$ for a sample of 87 SDSS FSRQs based on the spectral analysis of a larger FSRQs sample in Chen et al. (2009). The cosmological parameters $H_0 = 70 \text{ km s}^{-1} \text{ Mpc}^{-1}$, $\Omega_m = 0.3$, $\Omega_\Lambda = 0.7$ are used throughout the paper, and the spectral index is defined as $\alpha = f / \nu$ with f being the flux density at frequency ν .

2 SAMPLE AND DATA ANALYSIS

The parent sample of this work is 185 FSRQs in Chen et al. (2009). It was constructed through cross-correlating the Shen et al. (2006) SDSS DR3 X-ray quasar sample (3366 sources, see Shen et al. 2006 for details) with Faint Images of the Radio Sky at Twenty-Centimeters 1.4 GHz radio catalogue (FIRST, Becker, White & Helfand 1995) and the Green Bank 6 cm radio survey at 4.85 GHz radio catalogue (GB6, Gregory et al. 1996). The sample of 185 FSRQs was constructed from conventional definition of FSRQs with a spectral index between 1.4 and 4.85 GHz < 0.5 . In this work, we select 87 FSRQs with redshift $z < 0.83$ out of 185 FSRQs. The redshift restriction is selected in order to measure $[\text{O III}] 5007\text{\AA}$ line from SDSS spectra as well as $H\beta$.

The SDSS spectra cover the wavelength range from 3800 to 9200 \AA with a resolution of about 1800 - 2000 (see Schneider et al. 2005 for details). The spectral analysis is briefly described in this work, and more details can be found in Chen et al. (2009). The SDSS spectra were firstly corrected for the Galactic extinction using the reddening map of Schlegel, Finkbeiner & Davis (1998) and then shifted to their rest wavelength. We choose those wavelength ranges as pseudo-continua, which are not affected by prominent emission lines, and then decompose the spectra into the following three components: (1) A power-law continuum to describe the emission from the active nucleus. (2) An Fe II template adopting the UV Fe II template from Vestergaard & Wilkes (2001), and optical one from Véron-Cetty et al. (2004). (3) A Balmer continuum generated in the same way as Dietrich et al. (2002).

The modeling of above three components is performed by minimizing the χ^2 in the fitting process. The final multicomponent fit is then subtracted from the observed spectrum. The broad emission lines were measured from the continuum subtracted spectra. For the redshift range of our sources, we focused on several prominent emission lines, i.e. $H\beta$, $H\gamma$ and Mg II. Generally, two gaussian components were adopted to fit each of these lines, indicating the broad and narrow line components, respectively. The blended narrow lines, e.g. $[\text{O III}] 4959; 5007\text{\AA}$ and $[\text{He II}] 4686\text{\AA}$ blending with $H\beta$, and $[\text{S II}] 6716; 6730\text{\AA}$, $[\text{N II}] 6548; 6583\text{\AA}$ and $[\text{O I}] 6300\text{\AA}$ blending with $H\gamma$, were included as one gaussian component for each line at the fixed line wavelength. The χ^2 minimization method was used in fits. The line width FWHM, line flux of broad $H\beta$, $H\gamma$, Mg II and narrow $[\text{O III}] 5007\text{\AA}$ lines were obtained from the final fits for our sample.

There are various empirical relations between the radius of broad line region (BLR) and the continuum (and/or broad line) lu-

minosity, which can be used to calculate the black hole mass in combination with the line width FWHM of broad emission lines. Since the continuum luminosity of FSRQs are usually contaminated by the non-thermal jet emission, we use the Vestergaard & Peterson (2006) method to calculate M_{BH} , which utilizes the FWHM and luminosity of broad $H\beta$:

$$M_{\text{BH}} = 4.68 \times 10^6 \left(\frac{L_{\text{H}\beta}}{10^{42} \text{ erg s}^{-1}} \right)^{0.63} \left(\frac{\text{FWHM}_{\text{H}\beta}}{1000 \text{ km s}^{-1}} \right)^2 M_{\odot} \quad (2)$$

In this work, we also calculate the BLR luminosity L_{BLR} following Celotti, Padovani & Ghisellini (1997) by scaling the strong broad emission lines $H\beta$, $H\gamma$ and Mg II to the quasar template spectrum of Francis et al. (1991), in which Ly α is used as a reference of 100. By adding the contribution of $H\beta$ with a value of 77, the total relative BLR flux is 555.77, of which $H\beta$ 22 and Mg II 34 (Celotti et al. 1997; Francis et al. 1991).

As shown in Chen et al. (2009), the spectral energy distribution (SEDs) were constructed for each source using the radio FIRST 1.4 GHz and GB6 4.85 GHz data, the optical data selected as the line-free spectral region from SDSS spectra, and 1keV X-ray data compiled in Shen et al. (2006) from ROSAT All Sky Survey. When available, the 2MASS IR ($J; H; K_s$) (Skrutskie et al. 2006) and the Far- and near-UV GALEX data (Martin et al. 2005) are also added. The synchrotron peak frequency and the corresponding peak luminosity were thus obtained for each source through fitting the SED with a third-degree polynomial following Fossati et al. (1998). The thermal emission from accretion disk and host galaxy is estimated in Chen et al. (2009). The accretion disk emission is calculated assuming a steady geometrically thin, optically thick accretion disk around a Schwarzschild black hole and using estimated black hole mass and bolometric luminosity. The host galaxy spectra is estimated using the elliptical galaxy template of Mannucci et al. (2001), in combination with the bulge absolute luminosity in R-band estimated from $M_{\text{BH}} - M_{\text{R}}$ relation of McLure et al. (2004). The total contribution of accretion disk and host galaxy thermal emission are estimated by calculating the fraction of the thermal emission to the SED data at SDSS optical and GALEX UV region. A marginal value of 50% at most of SED wavebands is used to divide the FSRQs into thermal-dominated ($> 50\%$) and nonthermal-dominated ($< 50\%$). Using this criterion, 36 of 87 FSRQs in this work are non-thermal dominant FSRQs, and 51 are thermal-dominated ones. The $[\text{O III}]$ measurements are finally performed in 81 FSRQs, and $[\text{O III}]$ line is rather weak in remaining 6 FSRQs, which therefore can not be properly measured. Among 81 $[\text{O III}]$ available FSRQs, 32 sources are non-thermal dominant FSRQs, and 49 are thermal-dominated FSRQs.

3 RESULTS AND DISCUSSION

3.1 $M_{\text{bh}} - \sigma_{\text{[O III]}}$ relation

The relationship between the black hole mass M_{bh} and velocity dispersion $\sigma_{\text{[O III]}} = \text{FWHM}_{\text{[O III]}}/5007\text{\AA} = 2.35$ for all 81 FSRQs is shown in Fig. 1, in which the Tremaine et al. relation of equation (1) is also plotted as dashed line. From the figure, the significant scatter and deviation from Tremaine et al. relation is apparently seen, with majority of sources lying above the relation, which implies a higher black hole mass for our FSRQs than nearby inactive galaxies at given velocity dispersion. This result is actually consistent with Liu & Jiang (2006) and Bian et al. (2008) for general radio-loud AGNs/quasars. Both works claimed that radio-quiet AGNs even follow the Tremaine et al. $M_{\text{bh}} - \sigma_{\text{[O III]}}$ relation,

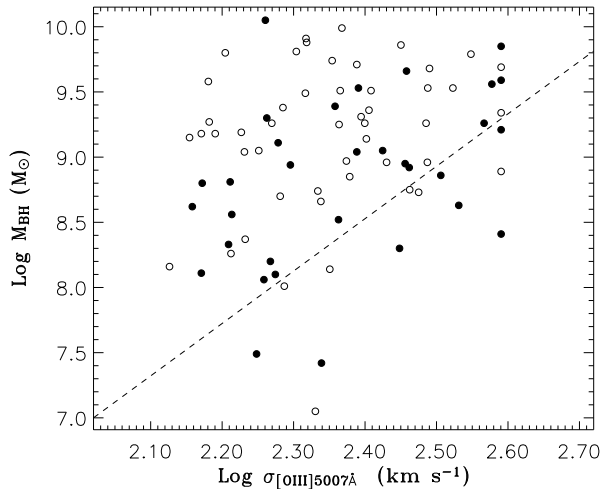


Figure 1. The velocity dispersion $\sigma_{[\text{O III}]}$ versus black hole mass. The dashed line is the M_{bh} relation of Tremaine et al. (2002) for 31 nearby inactive galaxies. The solid circles are non-thermal dominant FSRQs, while the open circles are thermal-dominant FSRQs.

however, radio-loud ones deviate with the same trend as ours. Alternatively, radio-loud quasars are found to have relatively smaller [O III] line width than radio quiet quasars at given black hole mass or bulge luminosity (e.g. Shields et al. 2003; Bonning et al. 2005). However, the reason is still unknown.

The relation between the BLR radius and $H\beta$ luminosity, and the corresponding empirical relation to estimate black hole mass in equation (2), are basically scaled from the AGNs sample with reverberation mapping black hole mass, of which most of sources are radio-quiet. The main advantage of equation (2) in estimating black hole mass for FSRQs is that the contamination of non-thermal jet emission (likely Doppler boosted) in continuum luminosity can be avoided. However, it is not proved yet whether it is applicable to radio-loud AGNs. As an evaluation of jet emission contamination, Liu et al. (2006) shown that the optical continuum luminosity of FSRQs usually exceed the value estimated from the $L_{\text{H}} - L_{5100\text{\AA}}$ relation $L_{5100\text{\AA}} = 0.843 \cdot 10^{-0.998} L_{\text{H}}^{0.998}$ fitted for Kaspi et al. (2000) radio quiet AGNs using ordinary least-square (OLS) linear fit method (see Fig. 4 in Liu et al. 2006). This result is consistent with the expectation that the continuum emission of FSRQs are contaminated by the (even dominant) non-thermal jet emission. As a check for our FSRQs sample, we plot the relationship between L_{H} and $L_{5100\text{\AA}}$ in Fig. 2. We found that the thermal FSRQs well follow the $L_{\text{H}} - L_{5100\text{\AA}}$ relation for radio quiet AGNs of Liu et al. (2006), supporting the dominance of thermal emission in these 51 FSRQs. However, large scatter exist for 36 nonthermal FSRQs. While most sources follow the relation, about 10 of 36 sources deviate from the relation, with larger luminosity at 5100\AA than expectations from relation, which is most likely due to the contribution of non-thermal jet emission.

The consistence of $L_{\text{H}} - L_{5100\text{\AA}}$ relation of the thermal-dominant FSRQs with that of radio quiet AGNs implies that the thermal continuum emission and the broad line emission follow the similar relation. Therefore, there will be likely little problem in estimating the BLR radius using empirical $L_{\text{H}} - R_{\text{BLR}}$ relation, unless the BLR kinematics (e.g. BLR radius) in our FSRQs is largely different from that of radio quiet AGNs. However, it is rather difficult to move our sources downward to follow the Tremaine et al. relation solely by changing BLR radius, let alone

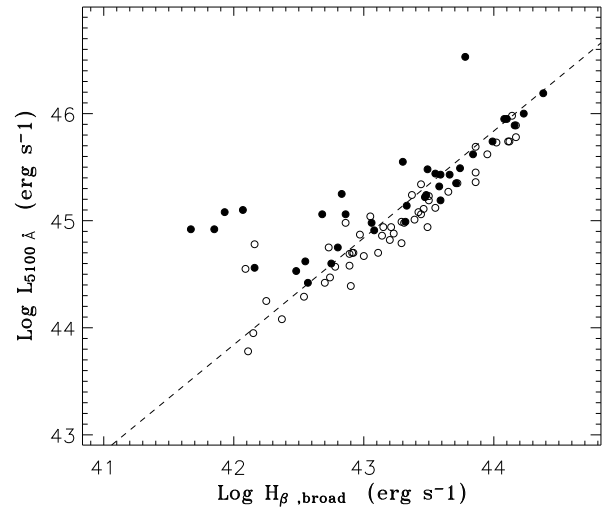


Figure 2. The luminosity at 5100\AA versus broad $H\beta$ luminosity. The symbols are same as in Fig. 1. The dashed line is the OLS bisector linear fit to Kaspi et al. (2000) radio quiet AGNs (see Liu et al. 2006).

to reduce the large scatter in Fig. 1. For radio-loud quasars, especially FSRQs, the disk-like BLR geometry (Wills & Browne 1986) can cause the underestimate of black hole mass (Lacy et al. 2001; McLure & Dunlop 2001). However, this effect will even make situation more sever, i.e. our FSRQs will deviate towards larger black hole mass from the Tremaine et al. relation. The likely explanation of smaller [O III] line width in radio-loud quasars can be a different [O III] kinematics or geometry in radio-loud quasars, especially for our FSRQs. However, the reason is unclear. The clues, if any, may be from the recent finding that the [O III] luminosity is not emitted isotropically and that there is significant extinction towards or within the narrow line region in a subset of Seyfert 2 galaxies, in the way that the observed [O III] luminosity are systematically smaller for obscured Seyferts by comparing [O III] with [O IV] $25.9 \mu\text{m}$ for a unbiased Seyfert galaxies sample (Diamond-Stanic et al. 2009; see also Jackson & Browne 1990; Hass et al. 2005; Meléndez et al. 2008; Zhang et al. 2008). More relevant to our FSRQs as radio powerful sources, the [O III] emission from quasars was compared with radio galaxies by Jackson & Browne (1990), and they found that the [O III] emission of quasars is much stronger than that of radio galaxies, which was interpreted as part of the [O III] emission being obscured by the torus in radio galaxies. The similar conclusion was reached by Haas et al. (2005) by comparing [O III] with [O IV] $25.9 \mu\text{m}$ for a sample of seven 3CR FR II radio galaxies and seven 3CR quasars. It is well established that the NLR is stratified with high-density and high ionization gas at close to the continuum source whereas low density and low-ionization gas is in the outer part of the NLR (Nagao et al. 2003; Riffel et al. 2006). Zhang et al. (2008) claimed that a significant fraction of the [O III] emission, at least for their Seyfert galaxies, may arise from the inner dense part of the NLR, which however can be covered thus obscured by the torus with its inner edge on scales of parsecs, and its extent likely on scales of several tens of parsecs (e.g., Schmitt et al. 2003, Jaffe et al. 2004). Due to the complex of [O III] line profile (Bonning et al. 2005), nevertheless, it needs further investigation on the M_{bh} relation for our FSRQs using other narrow lines, e.g. [S II] (Greene & Ho 2005). However, the redshift range will be much limited.

Although the detailed reason is unclear, the deviation of our FSRQs in Fig. 1 could be related with several recent findings on

the bulge - black hole relations (e.g., Aller & Richstone 2007; Hopkins et al. 2007; Lauer et al. 2007). The black hole masses predicted from the M_{bh} relation are found to be in conflict with those from the $M_{\text{bh}} - L_{\text{bulge}}$ relation for high-luminosity galaxies (e.g. brightest cluster galaxies: BCGs), with the former relation predicting a larger black hole mass (Lauer et al. 2007). While this may be explained by the slow increase in σ with L_{bulge} and the more rapid increase in effective radii with L_{bulge} seen in BCGs as compared to less luminous galaxies, the authors argued that the $M_{\text{bh}} - L_{\text{bulge}}$ relationship is a plausible description for galaxies of high luminosity. From the major galaxy merger simulations, Hopkins et al. (2007) found the so-called black hole mass fundamental plane in the form of $M_{\text{bh}} / M^{0.54} \sigma^{0.17} r^{2.2} \approx 0.5$, similar to relations found observationally, where M is the stellar mass. They also claimed that this fundamental plane is better than any single-variate predictor of black hole mass, e.g. the M_{bh} relation and the $M_{\text{bh}} - \sigma$ relation. Moreover, the bulge gravitational binding energy E_g may play a dominant role, in that $M_{\text{bh}} / E_g^{0.6}$ as found by Aller & Richstone (2007), which is as strong a predictor of M_{bh} as the velocity dispersion σ , for the elliptical galaxies. In view of these findings, it is possible that our FSRQs, especially those with high black hole mass (e.g. $M_{\text{bh}} > 3 \times 10^8 M_{\odot}$), may have larger bulge mass at a given σ . Alternatively, if these objects lie in the center of galaxies that continue to accrete the surrounding ICM after the initial black hole growth, as in so-called radio-mode feedback models (e.g., Croton et al., 2006), then perhaps the black hole can grow to a higher mass than the mass when it originally settled on the $M_{\text{bh}} - \sigma$ relationship. As shown in Croton et al. (2006) (see their Fig. 3.), the growth of black holes is dominated by the ‘quasar mode’ at high redshift and falls off sharply at $z \approx 2$, in contrast, the ‘radio mode’ becomes important at low redshifts where it suppresses cooling flows.

The deviation of M_{bh} from Tremaine et al. relation can be calculated as $M_{\text{bh}} = M_{\text{bh}}^{\text{pred}} (L_{\text{[O III]}})$, of which $M_{\text{bh}}^{\text{pred}} (L_{\text{[O III]}})$ is the predicted black hole mass from equation (1) using [O III] velocity dispersion. We perform the correlation analysis between M_{bh} and other parameters, i.e. redshift, Eddington ratio $L_{\text{bol}}/L_{\text{Edd}}$, 5 GHz luminosity $L_{5\text{GHz}}$, and synchrotron peak luminosity L_{peak} , and only found a moderately significant correlation between M_{bh} and redshift with Spearman correlation coefficient $r = 0.296$ at confidence level 99.3% . However, this correlation may likely be caused by the common dependence of other parameters, e.g. L_{H} . Indeed, the partial Spearman correlation analysis shown that the strong correlation no longer exist independent of L_{H} . Therefore, there is no strong evidence of cosmology evolution of $M_{\text{bh}} - L_{\text{[O III]}}$ relation up to $z = 0.83$. This is in contrast to the results of several studies (e.g. Woo et al. 2006; Shields et al. 2006) that have found apparent positive correlations between the M_{bh} relation and redshift. However, Shields et al. (2003) and Salvander et al. (2006), found no evidence for redshift evolution up to $z \approx 3$, using [O III] line widths as surrogates for σ .

3.2 Synchrotron peak luminosity, broad and narrow line region luminosity

The broad and narrow emission lines are believed to be produced from photonization process, although the shock-excitation from jet-ISM interaction can not be ignored for narrow emission lines in some AGNs (e.g. Dopita & Sutherland 1995). Therefore, the intimate relation is expected between broad and narrow line luminosities. Indeed, a significant correlation between the [O III] luminosity and BLR one is found with Spearman correlation coefficient

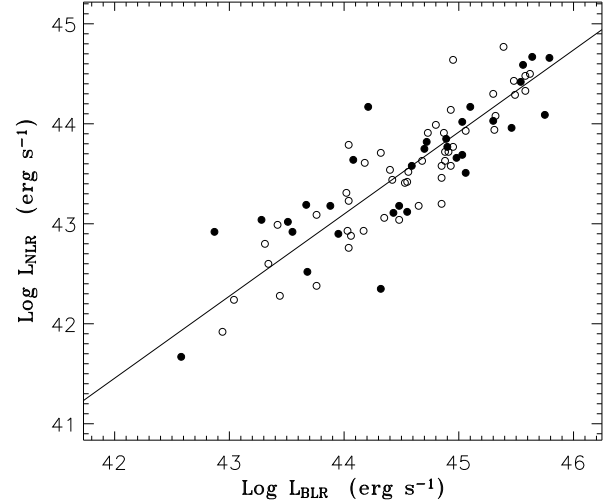


Figure 3. The BLR luminosity versus NLR luminosity. The symbols are same as in Fig. 1. The solid line is the OLS bisector linear fit for all 81 FSRQs.

$r = 0.875$ at confidence level of 99.99% . Using partial Spearman correlation analysis to exclude the common dependence of both luminosities on redshift, the correlation is still significant with correlation coefficient $r = 0.664$ at confidence level of 99.99% .

In this work, we tentatively transfer the [O III] 5007Å luminosity to NLR luminosity, using relation of $L_{\text{NLR}} = 3 (3 L_{\text{[O III]}} + 1.5 L_{\text{[O III]}})$ and assuming $L_{\text{[O III]}} = 4 L_{\text{[O II]}}$ (Rawlings & Saunders 1991). The relationship between the luminosity of BLR and NLR is presented in Fig. 3. The ordinary least-square (OLS) bisector linear fit to $L_{\text{BLR}} - L_{\text{NLR}}$ relation gives:

$$\log L_{\text{NLR}} = (0.89 \pm 0.05) \log L_{\text{BLR}} + (3.91 \pm 2.10) \quad (3)$$

The mean value of $\log L_{\text{NLR}}$ is $\langle \log L_{\text{NLR}} \rangle = 43.52 \pm 0.66$, and for $\log L_{\text{BLR}}$ is $\langle \log L_{\text{BLR}} \rangle = 44.53 \pm 0.75$. The BLR luminosity is, on average, larger than NLR luminosity by about one order of magnitude with $\langle \log (L_{\text{BLR}}/L_{\text{NLR}}) \rangle = 1.01 \pm 0.37$. This result means that the covering factor of NLR is about one tenth of that of BLR. Moreover, it is consistent within a factor of three with the ratio of BLR to NLR luminosities (≈ 25) calculated by using the relative flux in the composite quasar spectrum of Francis et al. (1991), which shows that our FSRQs spectra generally follow the composite spectrum although they are radio powerful sources. In addition, the scaling between the BLR and NLR luminosities enables us to statistically estimate the bolometric luminosity from narrow emission lines, which can be more readily observed, e.g. for type 2 AGNs. If using $L_{\text{bol}} = 30 L_{\text{BLR}}$ newly calibrated in Xu, Cao & Wu (2009), statistically, the bolometric luminosity can be estimated as $L_{\text{bol}} = 300 L_{\text{NLR}}$, i.e. $L_{\text{bol}} = 2025 L_{\text{[O III]}}$, implying a covering factor of 0.003 for narrow line region, similar to those of Rawlings & Saunders (1991) (0.01) and Willott et al. (1999) (0.003). More specifically, the calibration between the bolometric luminosity and NLR luminosity can be given through OLS bisector linear fit:

$$\log L_{\text{bol}} = (1.12 \pm 0.06) \log L_{\text{NLR}} + (3.92 \pm 2.59) \quad (4)$$

Our bolometric correction is consistent with Heckman et al. (2004) ($L_{\text{bol}}/L_{\text{[O III]}} \approx 3500$ for Seyfert galaxies with a scatter of approximately 0.38 dex) and Willott et al. (1999) ($L_{\text{bol}} \approx 5 \times 10^3 L_{\text{[O II]}}$). The consistent results are also recently found by Wu (2009b) that $L_{\text{bol}} / L_{\text{[O III]}}^{0.95} \approx 0.08$ for a sample of Seyfert 1 galax-

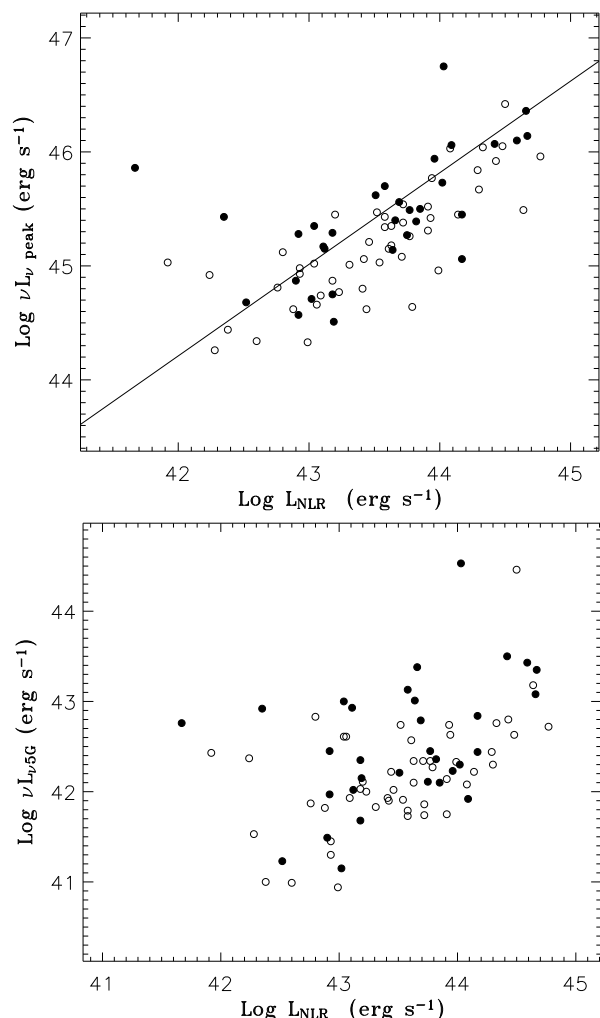


Figure 4. The upper panel: The synchrotron peak luminosity versus NLR luminosity. The symbols are same as in Fig. 1. The solid line is the OLS bisector linear fit for 32 non-thermal dominant FSRQs. The lower panel: 5 GHz luminosity versus NLR luminosity. The symbols are same as in Fig. 1.

ies and radio-quiet quasars using $L_{\text{bol}} = 9 L_{\text{5100\AA}}$, and the mean bolometric correction $L_{\text{bol}} = L_{\text{[O III]}} + 3400, 2000$ for 23 radio-quiet quasars and 20 Seyfert 1 galaxies, respectively.

The relationship between the NLR luminosity and synchrotron peak luminosity is given for all 81 FSRQs in Fig. 4. We found a strong correlation between two parameters with a Spearman correlation coefficient $r = 0.735$ at confidence level 99.99% . The partial correlation analysis gives a significant correlation with correlation coefficient $r = 0.408$ at confidence level 99.98% independent of redshift. When only 32 non-thermal dominant FSRQs are considered, the original significant correlation ($r = 0.637$ at confidence level 99.96%) still remains ($r = 0.406$ at confidence level 98%). For these 32 non-thermal dominant FSRQs, the OLS bisector linear fit on $L_{\text{peak}} - L_{\text{NLR}}$ relation gives:

$$\log L_{\text{peak}} = (0.80 \pm 0.10) \log L_{\text{NLR}} + (10.46 \pm 4.32) \quad (5)$$

which remains same when fitting on all 81 FSRQs. The strong correlation is also found between the NLR and 5 GHz luminosity (see Fig. 4), however, it is less significant ($r = 0.463$ at confidence level 99.99%) than that between the NLR luminosity and synchrotron peak luminosity.

The advantages of using the synchrotron peak luminosity is that the most of synchrotron emission are radiated at synchrotron peak frequency, at which the luminosity can be a good indicator of synchrotron emission. Since the synchrotron peak frequency varies from source to source, the luminosity at fixed waveband is actually from the different portion of source SED. This can be strengthened from Fig. 4, in which the large scatter in $L_{\text{5G}} - L_{\text{NLR}}$ is significantly reduced in $L_{\text{peak}} - L_{\text{NLR}}$, and with the less significance of the former correlation. This not only implies a tight relation between jet physics and accretion process, but also claims that the synchrotron peak luminosity can be a better indicator of jet emission than 5 GHz one. However, the possibility that part, if not all, of the $L_{\text{peak}} - L_{\text{NLR}}$ correlation can be caused from shock-excitation for NLR by the jet-ISM interactions (e.g. Dopita & Sutherland 1995; Bicknell et al. 1997), can not be completely excluded. By comparing the [O IV] 25.9 μm and [O III] luminosities for the combined sample of radio loud and radio quiet Seyfert galaxies, Meléndez et al. (2008) found that radio loud sources exhibit higher emission-line luminosities than those of radio quiet ones. The authors claimed that this result could be explained by a proposed bow shock model where part of the NLR emission is being powered by radio-emitting jets, present in radio-loud AGNs. Moreover, the jet-ISM interaction are invoked to explain the highly broadened [O III] line profiles in young radio galaxies (CSS/GPS sources) and some luminous linear radio sources (e.g., Gelderman & Whittle 1994; Nelson & Whittle 1996).

Although it can be a good indicator of the jet emission, the defect of the synchrotron peak luminosity lies in the contamination from beaming effect, which precludes it to well indicate the intrinsic source power. Only when the Doppler boosting is known for each source, the intrinsic source power can be obtained, which however can not be performed at present stage.

ACKNOWLEDGEMENTS

We thank the anonymous referee for insightful comments and constructive suggestions. We thank Qingwen Wu for valuable discussions. This work is supported by National Science Foundation of China (grants 10633010, 10703009, 10833002, 10773020 and 10821302), 973 Program (No. 2009CB824800), and the CAS (KJCX2-YW-T03).

Funding for the SDSS and SDSS-II has been provided by the Alfred P. Sloan Foundation, the Participating Institutions, the National Science Foundation, the U.S. Department of Energy, the National Aeronautics and Space Administration, the Japanese Monbukagakusho, the Max Planck Society, and the Higher Education Funding Council for England. The SDSS Web Site is <http://www.sdss.org/>. The SDSS is managed by the Astrophysical Research Consortium for the Participating Institutions. The Participating Institutions are the American Museum of Natural History, Astrophysical Institute Potsdam, University of Basel, University of Cambridge, Case Western Reserve University, University of Chicago, Drexel University, Fermilab, the Institute for Advanced Study, the Japan Participation Group, Johns Hopkins University, the Joint Institute for Nuclear Astrophysics, the Kavli Institute for Particle Astrophysics and Cosmology, the Korean Scientist Group, the Chinese Academy of Sciences (LAMOST), Los Alamos National Laboratory, the Max-Planck-Institute for Astronomy (MPIA), the Max-Planck-Institute for Astrophysics (MPA), New Mexico State University, Ohio State University, University of Pittsburgh, University of Portsmouth, Princeton University, the

United States Naval Observatory, and the University of Washington.

REFERENCES

- Aller M. C., Richstone D. O., 2007, *ApJ*, 665, 120
 Becker R. H., White R. L., Helfand D. J., 1995, *ApJ*, 450, 559
 Bian W., Zhao Y., 2004, *MNRAS*, 347, 607
 Bian W. H., Chen Y., Hu C., Huang K., Xu Y., 2008, *Chinese J. Astron. Astrophys.*, 8, 522
 Bicknell G. V., Dopita M. A., O’Dea C. P. O., 1997, *ApJ*, 485, 112
 Bonning E. W., Shields G. A., Salviander S., McLure R. J., 2005, *ApJ*, 626, 89
 Celotti A., Padovani P., Ghisellini G., 1997, *MNRAS*, 286, 415
 Chen Z. Y., Gu M. F., X. Cao, 2009, *MNRAS*, arXiv: 0904.1452
 Croton D. J. et al., 2006, *MNRAS*, 365, 11
 Diamond-Stanic A. M., Rieke G. H., Rigby J. R., 2009, *ApJ*, arXiv: 0904.0250
 Dietrich M., Appenzeller I., Vestergaard M., Wagner S. J., 2002, *ApJ*, 564, 581
 Dopita M. A., Sutherland R. S., 1995, *ApJ*, 455, 468
 Ferrarese L., Merritt D., 2000, *ApJ*, 539, L9
 Ferrarese L., Pogge R. W., Peterson B. M., Merritt D., Wandel A., Joseph C. L., 2001, *ApJ*, 555, L79
 Fossati G., Maraschi L., Celotti A., Comastri A., Ghisellini G., 1998, *MNRAS*, 299, 433
 Francis P. J., Hewett P. C., Foltz C. B., Chaffee F. H., Weymann R. J., Morris S. L., 1991, *ApJ*, 373, 465
 Gebhardt K. et al., 2000a, *ApJ*, 539, L13
 Gebhardt K. et al., 2000b, *ApJ*, 543, L5
 Gelderman R., Whittle M., 1994, *ApJS*, 91, 491
 Gregory P. C., Scott W. K., Douglas K., Condon J. J., 1996, *ApJS*, 103, 427
 Greene J. E., Ho L. C., 2005, *ApJ*, 627, 721
 Haas M., Siebenmorgen R., Schulz B., Krügel E., Chini R., 2005, *A&A*, 442, L39
 Heckman T. M., Kauffmann G., Brinchmann J., Charlot S., Tremonti C., White S. D. M., 2004, *ApJ*, 613, 109
 Hopkins P. F., Hernquist L., Cox T. J., Robertson B., Krause E., 2007, *ApJ*, 669, 45
 Jackson N., Browne I. W. A., 1990, *Nature*, 343, 43
 Jaffe A. H. et al., 2004, *ApJ*, 615, 55
 Kaspi S., Smith P. S., Netzer H., Maoz D., Jannuzi B. T., Giveon U., 2000, *ApJ*, 533, 631
 Kong M. Z., Wu X. B., Wang R., Han J. L., 2006, *Chinese J. Astron. Astrophys.*, 6, 396
 Kormendy J., Richstone D., 1995, *ARA&A*, 33, 581
 Lacy M., Laurent-Muehleisen S. A., Ridgway S. E., Becker R. H., White R. L., 2001, *ApJ*, 551, L17
 Lauer T. R. et al., 2007, *ApJ*, 662, 808
 Liu Y., Jiang D. R., 2006, *Chinese J. Astron. Astrophys.*, 6, 655
 Liu Y., Jiang D. R., Gu M. F., 2006, *ApJ*, 637, 669
 Magorrian J. et al., 1998, *AJ*, 115, 2285
 Mannucci F., Basile F., Poggianti B. M., Cimatti A., Daddi E., Pozzetti L., Vanzi L., 2001, *MNRAS*, 326, 745
 Martin D. C., Fanson J., Schiminovich D., Morrissey P., 2005, *ApJ*, 619, L1
 McLure R. J., Dunlop J. S., 2001, *MNRAS*, 327, 199
 McLure R. J., Willott C. J., Jarvis M. J., Rawlings S., Hill G. J., Mitchell E., Dunlop J. S., Wold M., 2004, *MNRAS*, 351, 347
 Meléndez M. et al., 2008, *ApJ*, 682, 94
 Nagao T., Murayama T., Shioya Y., Taniguchi Y., 2003, *AJ*, 126, 1167
 Nelson C. H., Whittle M., 1996, *ApJ*, 465, 96
 Nelson C. H., 2000, *ApJ*, 544, L91
 Rawlings S., Saunders R., 1991, *Nature*, 349, 138
 Riffel R., Rodríguez-Ardila A., Pastoriza M. G., 2006, *A&A*, 457, 61
 Salviander S., Shields G. A., Gebhardt K., Bonning E. W., 2006, *New Astron. Rev.*, 50, 803
 Salviander S., Shields G. A., Gebhardt K., Bonning E. W., 2007, *ApJ*, 622, 131
 Schlegel D. J., Finkbeiner D. P., Davis M., 1998, *ApJ*, 500, 525
 Schmitt H. R., Donley J. L., Antonucci R. R. J., Hutchings J. B., Kinney A. L., Pringle J. E., 2003, *ApJ*, 597, 768
 Schneider D. P. et al., 2005, *AJ*, 130, 367
 Shen J. J., Vanden Berk D. E., Schneider D. P., Hall P. B., 2008, *AJ*, 135, 928
 Shen S. Y., White S. D. M., Mo H. J., Voges W., Kauffmann G., Tremonti C., Anderson S. F., 2006, *MNRAS*, 369, 1639
 Shields G. A., Gebhardt K., Salviander S., Wills B. J., Xie B., Brotherton M. S., Yuan J., Dietrich M., 2003, *ApJ*, 583, 124
 Shields G. A., Menezes K. L., Massart C. A., Vanden Bout P., 2006, *ApJ*, 641, 683
 Skrutskie M. F. et al., 2006, *AJ*, 131, 1163
 Tremaine S. et al., 2002, *ApJ*, 574, 740
 Véron-Cetty M. P., Joly M., Véron P., 2004, *A&A*, 417, 515
 Vestergaard M., Wilkes B. J., 2001, *ApJS*, 134, 1
 Vestergaard M., Peterson B. M., 2006 *ApJ*, 641, 689
 Willott C. J., Rawlings S., Blundell K. M., Lacy M., 1999, *MNRAS*, 309, 1017
 Wills B. J., Browne I. W. A., 1986, *ApJ*, 302, 56
 Woo J.-H., Treu T., Malkan M. A., Blandford R. D., 2006, *ApJ*, 645, 900
 Wu Q. W., 2009a, *MNRAS*, submitted
 Wu Q. W., 2009b, *ApJ*, submitted
 Xu Y. D., Cao X., Wu Q. W., 2009, *ApJ*, 694, L107
 Zhang K., Wang T. G., Dong X. B., Lu H. L., 2008, *ApJ*, 685, L109